Regulation of α_{2B}-Adrenergic Receptor-mediated Extracellular Signal-regulated Kinase 1/2 (ERK1/2) Activation by ADP-ribosylation Factor 1*

Chunmin Dong[‡], Chunman Li[§], and Guangyu Wu[‡§1]

From the [‡]Department of Pharmacology and Experimental Therapeutics, Louisiana State University Health Sciences Center, New Orleans, Louisiana 70112 and the [§]Department of Pharmacology and Toxicology, Georgia Health Sciences University, Augusta, Georgia 30912

Background: ERK1/2 activation by G protein-coupled receptors can be mediated through multiple pathways.
Results: α_{2B}-Adrenergic receptor interacts with ADP-ribosylation factor 1 (ARF1) to modulate ERK1/2 activation.
Conclusion: ERK1/2 activation by α_{2B}-adrenergic receptor is mediated through a novel pathway involving ARF1.
Significance: The small GTPase ARF1 may function as an important regulator in receptor-mediated ERK1/2 activation.

A number of signaling molecules are involved in the activation of the mitogen-activated protein kinase (MAPK) pathway by G protein-coupled receptors. In this study, we have demonstrated that α_{2B}-adrenergic receptor (α_{2B}-AR) interacts with ADP-ribosylation factor 1 (ARF1), a small GTPase involved in vesicle-mediated trafficking, in an agonist activation-dependent manner and that the interaction is mediated through a unique double Trp motif in the third intracellular loop of the receptor. Interestingly, mutation of the double Trp motif and siRNA-mediated depletion of ARF1 attenuate α_{2B}-AR-mediated activation of extracellular signal-regulated kinases 1/2 (ERK1/2) without altering receptor intracellular trafficking, whereas expression of the constitutively active mutant ARF1Q71L and ARNO, a GDP-GTP exchange factor of ARF1, markedly enhances the activation of Raf1, MEK1, and ERK1/2. These data strongly demonstrate that the small GTPase ARF1 modulates ERK1/2 activation by α_{2B}-AR and provide the first evidence indicating a novel function for ARF1 in regulating the MAPK signaling pathway.

As the largest superfamily of cell surface receptors, G protein-coupled receptors (GPCRs)[2] regulate a variety of cellular functions largely through coupling to heterotrimeric G proteins, which in turn modulate the activity of downstream molecules, including adenylyl cyclases, phospholipases, protein kinases, and ion channels (1, 2). As the activation of the mitogen-activated protein kinase (MAPK) pathway is critically involved in the regulation of cell growth, survival, motility, and secretion, the mechanisms by which GPCRs activate MAPK have been intensively studied. The best characterized MAPK signaling cascade regulated by GPCRs involves sequential phosphorylation/activation of three protein kinases, Raf1, MEK1, and extracellular signal-regulated kinases 1/2 (ERK1/2). It has also been well recognized that the MAPK activation by GPCRs can be achieved through a number of distinct biochemical pathways, involving heterotrimeric G proteins, small GTPases, arrestins, and many protein kinases, and the predominant mechanism used depends upon receptor and cell types (3–10).

ADP-ribosylation factors (ARFs) belong to the superfamily of Ras-related small GTPases and modulate multiple intracellular trafficking processes (11). Like other Ras-related GTPases, ARF GTPases undergo recycling between their active GTP-bound and inactive GDP-bound conformations (12). Six ARF members have been identified in mammals, but ARF2 is not expressed in humans. Based on their sequences, ARF GTPases can be divided into Class I (ARF1–3), Class II (ARF4–5), and Class III (ARF6). Among these ARFs, ARF1, and ARF6 are the best characterized and most well understood members. Although ARF6 is involved in the regulation of actin cytoskeleton remodeling and endocytic and export trafficking (11, 13–15), ARF1 plays a crucial role in the formation of transport vesicles in the early and late secretory pathway. Activation of ARF1 GTPase controls the early secretory pathway through recruiting a complex of cytosolic proteins collectively known as coatomers, resulting in the formation of COPI-coated vesicles (16–18). ARF1 also regulates the targeting of clathrin to late Golgi and endosome compartments through recruiting the clathrin adaptor protein complex and Golgi-localized γ-ear-containing ARF1-binding proteins (GGAs) (19–21). In addition, ARF GTPases are able to activate phospholipase D, which may create lipid-enriched microdomains facilitating the recruitment of regulatory protein to the Golgi and promoting post-Golgi protein transport (22–26).

In this study, we have demonstrated that ARF1 interacts with a unique ditryptophan (diW) motif located in the third intracellular loop (ICL3) of α_{2B}-AR and modulates ERK1/2 activation by α_{2B}-AR. These data suggest a novel pathway in which α_{2B}-AR activates ERK1/2 via the small GTPase ARF1. These data also provide the first evidence implying an important role for ARF1 in the activation of the MAPK signaling pathway.

---

[1] To whom correspondence should be addressed: Dept. of Pharmacology and Toxicology, Georgia Health Sciences University, 1459 Laney Walker Blvd., Augusta, GA 30912. E-mail: guwu@georgiahealth.edu.
[2] The abbreviations used are: GPCR, G protein-coupled receptor; AR, adrenergic receptor; ARF, ADP-ribosylation factor; diW, double Trp; ICL, intracellular loop.

EXPERIMENTAL PROCEDURES

Materials—Antibodies were purchased from the following companies: ARF1 from StressGen (Ann Arbor, MI); ARF3 from BD Transduction Laboratories; phospho-Raf1 (Ser-338) from Upstate Biotech Millipore (Lake Placid, NY); GFP, phospho-ERK1/2, and Raf1 from Santa Cruz Biotechnology, Inc. (Santa Cruz, CA); HA-fluorescein (3F10) from Roche Diagnostics; ERK1/2, MEK1, and phospho-MEK1 (Thr-286) from Cell Signaling Technology, Inc. (Beverly, MA). The radioligand [³H]RX821002 (specific activity = 41 Ci/mmol) was purchased from PerkinElmer Life Sciences. All other materials were obtained as described elsewhere (27–29).

Plasmid Constructions—α_{2B}-AR tagged with GFP at its C terminus or three HAs at its N terminus was generated as described previously (27). A similar strategy was utilized to generate GFP-conjugated ARF1 using the BamHI and EcoRI restriction sites of the pEGFP-N1 vector. GST fusion proteins encoding the ICL3 of α_{2B}-AR were generated into the pGEX-4T-1 vector using a strategy as described previously (30, 31). The different regions of the α_{2B}-AR ICL3 were amplified by PCR and subcloned into the BamHI and XhoI restriction sites. The mutations were carried out using the QuikChange site-directed mutagenesis kit (Stratagene, La Jolla, CA). The sequence of each construct used in this study was verified by restriction mapping and nucleotide sequence analysis.

Cell Culture and Transient Transfection—HEK293 cells were cultured in Dulbecco's modified Eagle's medium (DMEM) with 10% fetal bovine serum, 100 units/ml penicillin, and 100 μg/ml streptomycin. The human breast cancer MCF-7 cells were cultured in RPMI 1640 medium supplemented with 10% fetal bovine serum, 2 mM glutamine, 1 mM sodium pyruvate, 100 units/ml penicillin, and 100 μg/ml streptomycin. Transient transfection of cells was carried out using Lipofectamine 2000 reagent (Invitrogen) as described previously (27). The transfection efficiency was estimated to be greater than 70% based on the GFP fluorescence.

Co-immunoprecipitation—For co-immunoprecipitation of α_{2B}-AR and ARF1, HEK293 cells cultured on 100-mm dishes were co-transfected with 2 μg of HA-tagged α_{2B}-AR and ARF1 for 36 h. After starvation for at least 3 h, the cells were stimulated with UK14,304 at a concentration of 1 μM for different time periods. The cells were then washed twice with PBS and harvested and lysed with 500 μl of lysis buffer containing 50 mM Tris-HCl, pH 7.4, 150 mM NaCl, 1% Nonidet P-40, 0.5% sodium deoxycholate, 0.1% SDS, and Complete Mini protease inhibitor mixture. After gentle rotation for 1 h, samples were centrifuged for 15 min at 14,000 $\times$ g, and the supernatant was incubated with 50 μl of protein G-Sepharose for 1 h at 4 °C to remove nonspecific bound proteins. Samples were then incubated with 1 μg of anti-HA or anti-GFP antibodies overnight at 4 °C with gentle rotation followed by incubation with 50 μl of protein G-Sepharose 4B beads for 5 h. Resin was collected by centrifugation and washed three times with 500 μl of lysis buffer without SDS. Immunoprecipitated receptors were eluted with SDS gel loading buffer, separated by 10% SDS-PAGE, and visualized by immunoblotting using anti-HA antibodies (28). ARF1 in the immunoprecipitates was detected by using anti-ARF1 antibodies.

GST Fusion Protein Pulldown Assay—GST fusion proteins were expressed in bacteria and purified using a glutathione affinity matrix as described previously (30–32). GST fusion proteins immobilized on the glutathione resin were either used immediately or stored at 4 °C for no longer than 3 days. Each batch of fusion protein used in experiments was first analyzed by Coomassie Blue staining following SDS-PAGE. GST fusion proteins tethered to the glutathione resin were incubated with cell lysate prepared from HEK293 cells in 500 μl of binding buffer (20 mM Tris-HCl, pH 7.5, 2% Nonidet P-40, 70 mM NaCl) at 4 °C overnight. The resin was washed four times with 1 ml of binding buffer, and the retained proteins were solubilized in 1× SDS gel loading buffer and separated by SDS-PAGE. Bound proteins were detected by immunoblotting.

Radioligand Binding—Cell surface expression of α_{2B}-AR in HEK293 cells was measured by ligand binding of intact live cells using [³H]RX821002 as described previously (28). Briefly, HEK293 cells were cultured on 6-well dishes and transfected with 200 ng of the α_{2B}-AR plasmid. After 6 h, the cells were split into 12-well plates at a density of 4×10^5 cells/well and cultured for an additional 24 h. The cells were incubated with DMEM plus [³H]RX821002 at a concentration of 20 nM for 90 min at room temperature. The nonspecific binding was determined in the presence of rauwolscine (10 μM). The cells were washed twice with 1 ml of PBS, and the cell surface-bound ligands were extracted by 1 M NaOH treatment for 2 h. The radioactivity was counted by liquid scintillation spectrometry in 3.5 ml of Ecoscint A scintillation solution (National Diagnostics, Inc., Atlanta, GA).

For measurement of α_{2B}-AR internalization, HEK293 cells were cultured on 6-well dishes and transfected with 0.5 μg of α_{2B}-AR with or without co-transfection with 1 μg of arrestin-3 for 24 h. After starvation for 3 h, the cells were stimulated with epinephrine at a concentration of 100 μM for different time periods (9). The cells were washed three times with cold PBS, and α_{2B}-AR expression at the cell surface was measured by intact cell ligand binding as described above.

Flow Cytometric Analysis of Receptor Expression—α_{2B}-AR expression at the cell surface was also measured by flow cytometry as described previously (29, 33). HEK293 cells transfected with HA-α_{2B}-AR were suspended in PBS containing 1% FBS at a density of 4×10^6 cells/ml and incubated with high affinity anti-HA-fluorescein (3F10) at a final concentration of 2 μg/ml for 30 min at 4 °C. After washing twice with 0.5 ml of PBS, 1% FBS, the cells were resuspended, and the fluorescence was analyzed on a flow cytometer (BD Biosciences FACSCalibur). Because the staining with the anti-HA antibodies was carried out in the nonpermeabilized cells and only those receptors expressed at the cell surface were accessible to the anti-HA antibodies, the measured fluorescence reflected the amount of receptor expressed at the cell surface.

For measurement of overall α_{2B}-AR expression, HEK293 cells transfected with α_{2B}-AR-GFP were collected and resuspended in PBS containing 1% FBS at a density of 8×10^6 cells/ml. Total receptor expression was determined by measuring

GFP fluorescence on a flow cytometer as described previously (27).

Fluorescence Microscopy—HEK293 cells were grown on coverslips precoated with poly-L-lysine in 6-well plates and transfected with GFP-tagged α_{2B}-AR. The cells were fixed with 4% paraformaldehyde, 4% sucrose mixture in PBS for 15 min and stained with 4′,6-diamidino-2-phenylindole for 5 min. The coverslips were mounted, and fluorescence was detected with a Leica DMRA2 epifluorescence microscope. Images were deconvolved using SlideBook software and the nearest neighbor deconvolution algorithm (Intelligent Imaging Innovations, Denver, CO) as described previously (27, 28).

Measurement of Raf1, MEK1, and ERK1/2 Activation—HEK293 cells were cultured on 10-cm dishes and transfected with 2 μg of α_{2B}-AR plasmids with or without co-transfection with ARF1 siRNA. At 6–8 h after transfection, the cells were split into 6-well dishes and cultured for 24–30 h. The cells were starved for at least 2 h and then stimulated with UK14,304 as indicated in the legends for Figs. 1 and 3–6. Stimulation was terminated by the addition of 1× SDS gel loading buffer as described previously (27, 28). After solubilizing the cells, 20 μl of total cell lysates was separated by 12% SDS-PAGE. To determine the effect of transient expression of small GTPases on the MAPK activation, HEK293 cells cultured on 6-well dishes were transfected with 1.0 μg of individual GTPase for 24–36 h. Activation of Raf1, MEK1, and ERK1/2 was determined by immunoblotting measuring their phosphorylation with phospho-specific antibodies.

Measurement of cAMP Production—cAMP concentrations were measured by using cyclic AMP XP™ assay kit (Cell Signaling Technology). Briefly, HEK293 cells were cultured in 6-well dishes and transfected with 0.5 μg of α_{2B}-AR with or without co-transfection with control or ARF1 siRNA. The cells were then split into 96-well plates at a density of 1×10^4 cells/well. After starvation for 1 h, the cells were stimulated with forskolin at a concentration of 1 μM plus or minus different concentrations of UK14,304 (from 10 to 1000 nM) in the presence of 0.1 mM isobutylmethylxanthine for 5 min at 37 °C. The reactions were stopped by aspirating the medium, and then the cells were lysed with 100 μl of lysis buffer. Fifty μl of cell lysate was transferred into microtiter plates, and cAMP concentrations were measured according to the protocol provided by the kit. In each experiment, a standard curve was generated in parallel and used to calculate cAMP concentrations.

siRNA-mediated Knockdown of ARF1—Two Stealth™ RNAi duplexes targeting ARF1 (siRNA 1 5′-GGGAACAUCUUCGC-CAACCUCUUCA-3′ and siRNA 2 5′-ACAGCAAUGACA-GAGAGCGUGUGAA-3′) and a nonspecific duplex oligonucleotide (5′-GGGUACUUCCGCAACUCCUCAAUCA-3′) were obtained from Invitrogen. HEK293 cells were plated on 6-well dishes at a density of 4×10^5 cells/well for 12–16 h before transfection. α_{2B}-AR and siRNA were simultaneously transfected by using Lipofectamine 2000 reagent (27, 34). Briefly, 7.5 μl of Lipofectamine 2000 and 6 μl of 20 μM RNAi plus 0.5 μg of α_{2B}-AR were added separately into 100 μl of Opti-MEM medium. After a 5-min incubation, both solutions were mixed and incubated for 20 min. The transfection mixture was added to culture dishes containing 0.8 ml of fresh DMEM without
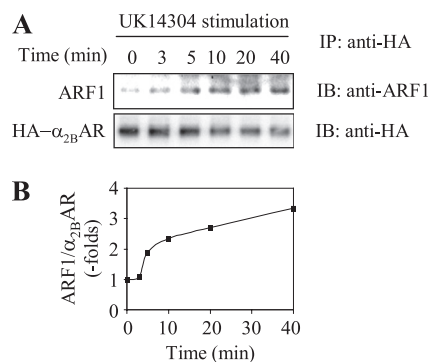

FIGURE 1. **Agonist activation-dependent association of α_{2B}-AR with ARF1.** *A*, HEK293 cells were transfected with HA-α_{2B}-AR and ARF1 and then stimulated with 1 μM UK14,304 for different time periods (0–40 min). HA-α_{2B}-AR was immunoprecipitated with anti-HA antibodies. ARF1 in the immunoprecipitates (*IP*) was detected by Western blotting (*IB*) using anti-ARF1 antibodies and HA-α_{2B}-AR by using anti-HA antibodies. *B*, quantitative data shown in *A*. Data shown are the ratio of α_{2B}-AR-associated ARF1 to the total α_{2B}-AR in the immunoprecipitates. Similar results were obtained in at least three individual experiments.

antibiotics. After incubation at 37 °C for 6–8 h, culture medium was changed to full DMEM. Similarly, MCF7 cells were transfected with control and ARF1 siRNA. All the experiments were performed at 48 h after RNAi transfection.

Immunoblotting—Western blot analysis of protein expression was carried out as described previously (27). HEK293 cell lysates were separated by SDS-PAGE and transferred onto polyvinylidene difluoride membranes. The signal was detected using ECL Plus (PerkinElmer Life Sciences) and a Fuji Film luminescent image analyzer (LAS-1000 Plus) and quantitated using the Image Gauge program (version 3.4).

Statistical Analysis—Differences were evaluated using Student's t test, and $p < 0.05$ was considered as statistically significant. Data are expressed as the mean ± S.E.

RESULTS

α_{2B}-AR Interacts with ARF1 in Response to Agonist Stimulation—HEK293 cells were transfected with HA-tagged α_{2B}-AR and ARF1 and stimulated with UK14,304 for different time periods (0–40 min). The interaction between α_{2B}-AR and ARF1 was measured by co-immunoprecipitation with anti-HA antibodies. A significant amount of ARF1 was found in the anti-HA immunoprecipitates, and stimulation with the agonist UK14,304 promoted α_{2B}-AR association with ARF1 in a time-dependent fashion. The maximal binding was observed after a 10-min stimulation (Fig. 1, *A* and *B*). These data indicate that activation of α_{2B}-AR enhances its interaction with ARF1 GTPase.

Identification of the ARF1-binding Motif in α_{2B}-AR—We next sought to identify the ARF1-binding site in α_{2B}-AR by focusing on the ICL3. The ICL3 is relatively larger (165 residues) (Fig. 2*A*) than other intracellular domains, and the ICL3 of M3-muscarinic receptor has been implicated in the interaction with ARF1 (35). The ICL3 was generated as a GST fusion protein, and its interaction with ARF1 was determined in the GST fusion protein pulldown assay. The GST fusion protein encoding the ICL3, but not GST, was able to interact with ARF1 (Fig. 2, *B* and *C*).

A α₂B-AR ICL3

```
205 KRSHCRGLGA KRGSGEGESK KPQPVAGGVP TSAKVPTLVS PLSSVGEANG
    HPKPPREKEE GETPEDPEAR ALPPTWSALP RSGQGQKKGT SGATAEEGDE
    EDEEEVEECE PQTLPASPAS VCNPPLQQPQ TSRVLATLRG QVLLGKNVGV
    ASGQWWRRRT QLSRE 369
```

B

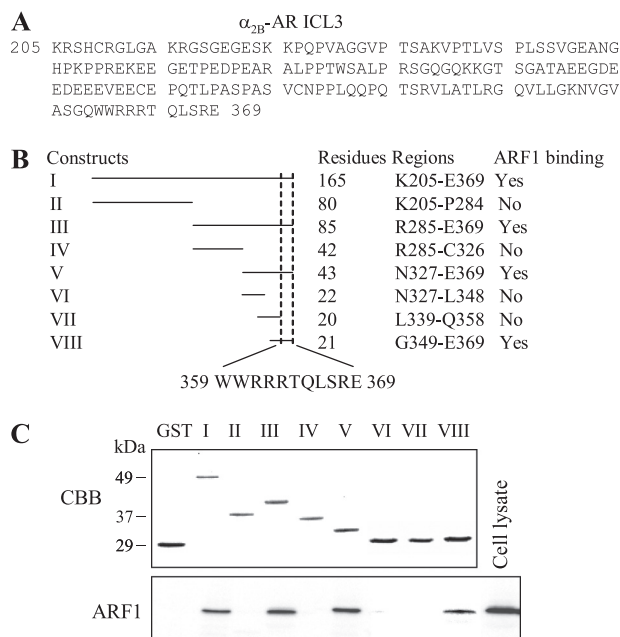| Constructs		Residues	Regions	ARF1 binding
I		165	K205-E369	Yes
II		80	K205-P284	No
III		85	R285-E369	Yes
IV		42	R285-C326	No
V		43	N327-E369	Yes
VI		22	N327-L348	No
VII		20	L339-Q358	No
VIII		21	G349-E369	Yes

359 WWRRRTQLSRE 369

C

FIGURE 2. **Identification of an ARF1-binding subdomain in the third intracellular loop of α₂B-AR by GST fusion protein pulldown assay.** *A*, sequence of the ICL3 of α₂B-AR generated as the GST fusion proteins. *B*, summary of progressive truncation of the ICL3 to identify the ARF1-binding subdomain in a GST fusion protein pulldown assay. *C*, the purified GST fusion proteins encoding different regions of the ICL3 of α₂B-AR (*upper panel*) and their interaction with ARF1 (*lower panel*). GFP-tagged ARF1 was expressed in HEK293 cells and total cell homogenates were incubated with GST fusion proteins as described under "Experimental Procedures." ARF1 interaction with the fusion proteins was revealed by immunoblotting using anti-GFP antibodies. *Upper panel*, Coomassie Brilliant Blue staining (*CBB*) of purified GST fusion proteins; *Lower panel*, GFP-ARF1 bound to the GST fusion proteins. These experiments were repeated at least six times with similar results. Molecular mass is indicated at the *left*.

We then utilized the progressive deletion strategy (Fig. 2*B*) to search for a subdomain in the ICL3 binding to ARF1. The GST fusion proteins encoding Arg-285–Glu-369, Asn-327–Glu-369, and Gly-349–Glu-369 interacted with ARF1, whereas GST fusion proteins encoding Lys-205–Pro-284, Arg-285–Cys-326, Asn-327–Leu-348, and Leu-339–Gln-358 were not able to bind ARF1 (Fig. 2, *B* and *C*). These data suggest that the ARF1-binding motif is localized in the C-terminal fragment WWRRRTQLSRE.

To precisely identify specific residues mediating the ICL3 interaction with ARF1, each of the residues in the ARF1-binding domain WWRRRTQLSRE (Fig. 3*A*) was mutated to Ala by site-directed mutagenesis using GST fusion protein encoding Gly-349–Glu-369 (construct VIII) as a template (Fig. 3*B*). Mutation of Trp-359 or Trp-360 significantly attenuated the ICL3 interaction with ARF1, and simultaneous mutation of Trp-359 and Trp-360 residues abolished the ICL3 interaction with ARF1, whereas mutation of Thr-364, Gln-365, Leu-366, Ser-367, Arg-368, Glu-369, and Arg-362/363/364 did not significantly reduce ARF1 interaction (Fig. 3*B*). These data demonstrate that the diW motif (Trp-359 and Trp-360) specifically mediates the interaction of the ICL3 with ARF1 GTPase *in vitro*.

We next determined whether the diW motif mediates the interaction of the full-length α₂B-AR with ARF1 in the absence and presence of agonist stimulation. HEK293 cells were trans-
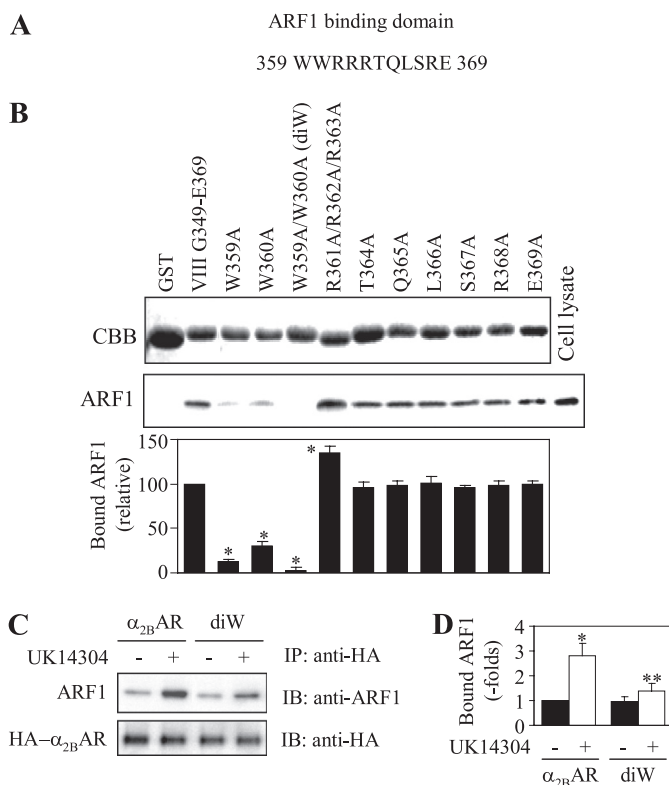
A ARF1 binding domain

359 WWRRRTQLSRE 369

B

C **D**

FIGURE 3. **The diW motif in the third intracellular loop mediates α₂B-AR interaction with ARF1.** *A*, sequence of an ARF1-binding domain in the ICL3 of α₂B-AR. *B*, effect of mutating individual residues in the ARF1-binding domain on the ICL3 interaction with ARF1. Each of the residues in the ARF1-binding domain was mutated to Ala and generated as GST fusion proteins (*upper panel*). Their interaction with ARF1 was determined by GST fusion protein pulldown assays as described in the legend for Fig. 2 (*middle panel*). *Lower panel*, quantitative data shown as the percentages of the ARF1 bound to the construct VIII Gly-349–Glu-369 and presented as the mean ± S.E. of three experiments. *, *p* < 0.05 *versus* the construct VIII. *CBB*, Coomassie Brilliant Blue staining. *C*, the diW motif specifically mediates α₂B-AR interaction with ARF1 in response to agonist stimulation. HEK293 cells were transfected with HA-α₂B-AR or its diW motif mutant and then stimulated with 1 μM UK14,304 for 5 min. α₂B-AR interaction with ARF1 was determined by co-immunoprecipitation using anti-HA antibodies as described in the legend for Fig. 1. *D*, quantitative data shown in *C*. Data shown are the ratio of α₂B-AR-associated ARF1 to the total α₂B-AR in the immunoprecipitates and presented as the mean ± S.E. (*n* = 3); *, *p* < 0.05 *versus* cells without agonist stimulation; **, *p* < 0.05 *versus* cells expressing wild-type α₂B-AR and stimulated with UK14,304.

fected with HA-tagged α₂B-AR or its diW motif mutant and stimulated with UK14,304. Consistently, the full-length α₂B-AR physically associated with ARF1 in the presence and absence of agonist, but the agonist stimulation profoundly enhanced the interaction (Fig. 3, *C* and *D*). Interestingly, the association of α₂B-AR with ARF1 was almost the same as its diW motif mutant at the basal level, whereas the interaction of the α₂B-AR mutant with ARF1 in response to the agonist UK14,304 stimulation was markedly reduced as compared with its wild-type counterpart (Fig. 3, *C* and *D*). These data demonstrate that the diW motif in the ICL3 specifically mediates the interaction of the agonist-activated α₂B-AR with ARF1 GTPase.

Role of the diW Motif-mediated α₂B-AR Interaction with ARF1 in ERK1/2 Activation—ARF1 has been well documented to play a crucial role in vesicle-mediated transport (11), and our previous studies have shown that expression of dominant-negative ARF1 mutants inhibits α₂B-AR transport to the cell surface (36). Therefore, as an initial approach to define the role of
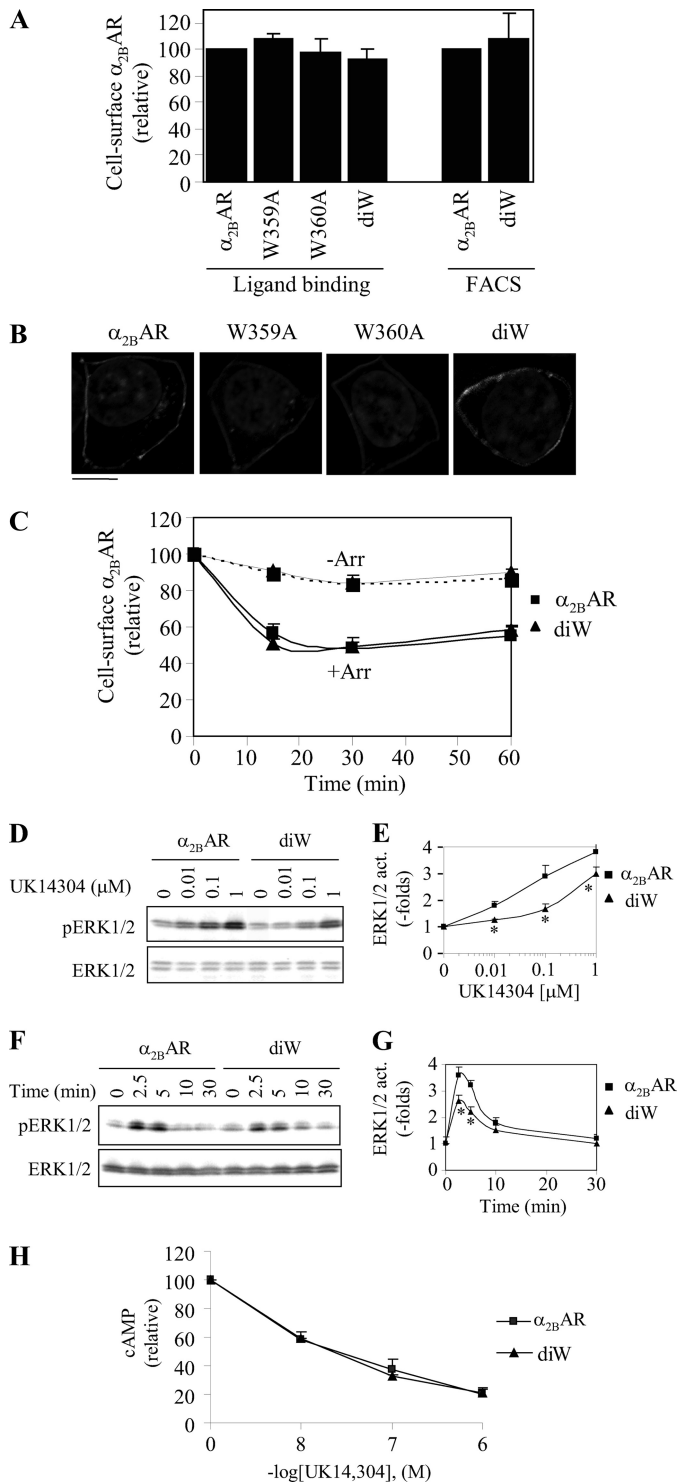
FIGURE 4. **Effect of mutating the diW motif on the intracellular trafficking of α_{2B}-AR and ERK1/2 activation by α_{2B}-AR.** *A*, cell surface expression of α_{2B}-AR and its diW motif mutants. *Left side*, α_{2B}-AR and its diW motif mutants were transiently expressed in HEK293 cells, and their expression at the cell surface was measured by intact cell ligand binding using [^{3}H]RX821002. The mean values of specific ligand binding were $17{,}642 \pm 1203$ cpm ($n = 6$, each in triplicate) from cells transfected with α_{2B}-AR. *Right side*, α_{2B}-AR and its diW motif mutant were tagged with HA at their N termini and expressed in HEK293 cells. The cell surface expression of the receptors was determined by flow cytometry following staining with anti-HA antibodies in nonpermeabilized cells. Data shown are the mean $\pm$ S.E. ($n = 4$) and presented as relative to wild-type α_{2B}-AR. *B*, subcellular localization of α_{2B}-AR and its diW motif mutant revealed by fluorescence microscopy detecting the GFP signal. The data are representative images of at least five independent experiments.

the diW motif-mediated α_{2B}-AR interaction with ARF1, we determined whether this interaction is required for export trafficking of newly synthesized receptor from the endoplasmic reticulum to the cell surface. Similar to wild-type α_{2B}-AR, the diW mutant normally transported to the cell surface as measured by intact cell ligand binding (Fig. 4*A*). To exclude the possible influence of the mutation on the ligand binding properties of the receptor, we also used flow cytometry to measure the cell surface expression of HA-tagged α_{2B}-AR and its diW mutant. Consistently, no significant difference was observed in the cell surface expression of α_{2B}-AR and its diW motif mutant (Fig. 4*A*). Consistent with the intact cell ligand binding and flow cytometry data, α_{2B}-AR and its mutants W359A, W360A, and W359A/W360A were similarly and robustly expressed at the cell surface (Fig. 4*B*).

A recent study has demonstrated that ARF1 also modulates protein transport from the plasma membrane to endosomes (37). Therefore, we next determined whether the diW motif-mediated α_{2B}-AR interaction with ARF1 modulates the endocytic trafficking of agonist-occupied α_{2B}-AR. The α_{2B}-AR diW motif mutant underwent internalization in response to the agonist UK14,304 stimulation at the level identical to its wild-type counterpart (Fig. 4*C*). Co-expression of arrestin-3, which has been demonstrated to facilitate α_{2B}-AR internalization (9), similarly potentiated the internalization of both α_{2B}-AR and its diW motif mutant (Fig. 4*C*). These data suggest that ARF1 interaction with α_{2B}-AR does not play a major role in intracellular trafficking, including cell surface transport and internalization, of the receptor.

We then determined whether the diW motif-mediated α_{2B}-AR interaction with ARF1 modulates α_{2B}-AR signaling by measuring ERK1/2 activation and cAMP inhibition following stimulation with UK14,304. Time- and agonist dose-dependent stimulation of ERK1/2 was significantly attenuated in cells expressing the diW mutant as compared with cells expressing wild-type α_{2B}-AR (Fig. 4, *D–G*). The EC_{50} values were 0.04 and 0.3 μM UK14,304 for α_{2B}-AR and its diW motif mutant, respec-

Scale bar, 10 μm. *C*, internalization of α_{2B}-AR and its diW motif mutant in the presence or absence of overexpressed arrestin-3. α_{2B}-AR or its diW motif mutant were expressed with (+*Arr*) or without (−*Arr*) arrestin-3 and then stimulated with epinephrine at a concentration of 100 μM for the indicated times. α_{2B}-AR expression at the cell surface was measured by intact cell ligand binding. Data shown are the mean $\pm$ S.E. ($n = 3$). *D* and *F*, effect of mutating the diW motif on ERK1/2 activation by α_{2B}-AR. HEK293 cells were transfected with α_{2B}-AR or its diW motif mutant and stimulated with increasing concentrations of UK14,304 for 5 min (*D*) or with 0.1 μM UK14,304 for different time periods (*F*). ERK1/2 activation was measured by Western blotting measuring their phosphorylation using phospho-specific anti-ERK1/2 antibodies. *Upper panel*, a representative blot of ERK1/2 activation; *Lower panel*, total ERK1/2 expression. *pERK1/2*, phosphorylated ERK1/2. *E* and *G*, quantitation of data shown in *D* and *F*, respectively. The data are expressed as -fold increase over the basal level and presented as the mean $\pm$ S.E. of three separate experiments. *, $p < 0.05$ *versus* cells transfected with α_{2B}-AR. *ERK1/2 act.*, ERK1/2 activation. *H*, effect of mutating the diW motif on cAMP inhibition by α_{2B}-AR. HEK293 cells were transfected with α_{2B}-AR or its diW motif mutant and stimulated with 1 μM forskolin plus different concentrations of UK14,304 for 5 min at 37 °C. Total cellular cAMP was measured by using the cyclic AMP XP™ assay kit as described under "Experimental Procedures." Basal cAMP concentrations were as follows: α_{2B}-AR, 16.5 ± 2.3 pmol/well; diW mutant, 17.0 ± 1.6 pmol/well. Forskolin-induced cAMP concentrations were as follows: α_{2B}-AR, 131.1 ± 15 pmol/well; diW mutant, 138.6 ± 14 pmol/well. The data shown are percentages of the mean value obtained from cells stimulated with forskolin alone and are presented as the mean $\pm$ S.E. of three experiments.
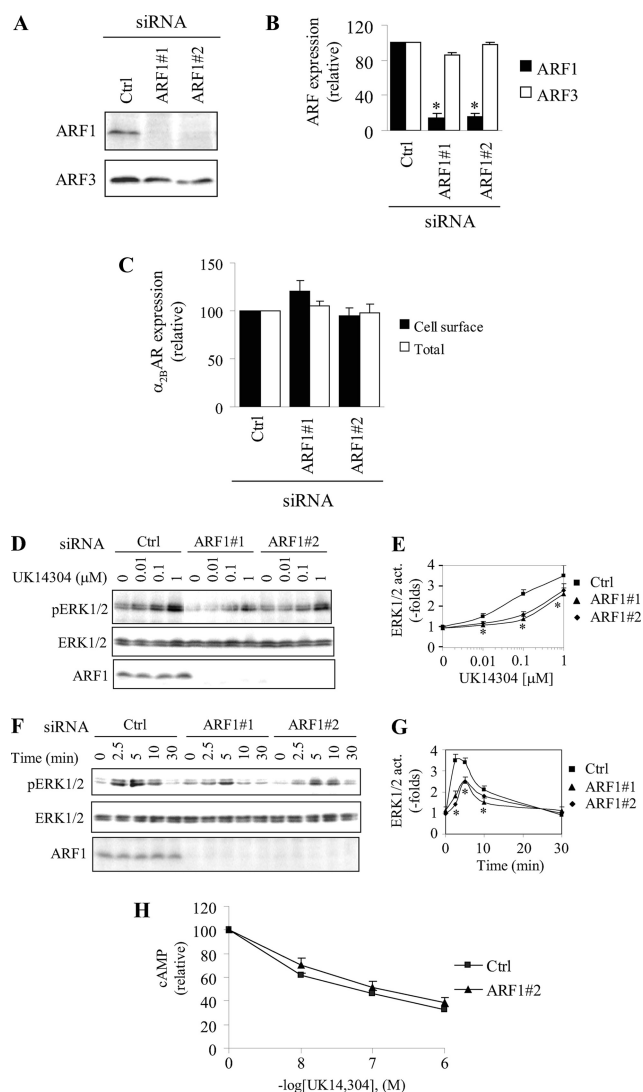
FIGURE 5. **Effect of siRNA-mediated knockdown of ARF1 on the cell surface expression of α_{2B}-AR and ERK1/2 activation by α_{2B}-AR.** A, HEK293 cells cultured on 6-well dishes were transiently transfected with control siRNA (Ctrl) or individual ARF1 siRNAs (ARF#1 and ARF#2) as described under "Experimental Procedures." At 48 h after transfection, total homogenate protein was separated by 12% SDS-PAGE, and expression of ARF1 (upper panel) and ARF3 (lower panel) was detected by Western blotting using isoform-specific antibodies. B, quantitation of data shown in A. The data are expressed as percentages of ARF1 and ARF3 expression in cells transfected with control siRNA and presented as the mean ± S.E. of three individual experiments. *, $p < 0.05$ versus control. C, effect of siRNA-mediated depletion of ARF1 on the cell surface expression of α_{2B}-AR. HEK293 cells were transfected with α_{2B}-AR together with the control or ARF1 siRNA, and the cell surface expression of α_{2B}-AR was determined by intact cell ligand binding as described in the legend for Fig. 4. The data shown are percentages of the mean value obtained from cells transfected with α_{2B}-AR and control siRNA and are presented as the mean ± S.E. of three experiments. D and F, effect of expression of ARF1 siRNA on ERK1/2 activation by α_{2B}-AR. HEK293 cells were transfected with α_{2B}-AR and control siRNA or individual ARF1 siRNA and stimulated with increasing concentrations of UK14,304 for 5 min (D) or with 0.1 μM UK14,304 for different time periods (F). ERK1/2 activation was measured by Western blotting measuring their phosphorylation using phospho-specific anti-ERK1/2 antibodies. Upper panel, a representative blot of ERK1/2 activation. Middle panel, total ERK1/2 expression. Lower panel, ARF1 expression. pERK1/2, phosphorylated ERK1/2. E and G, quantitative data showed in D and F, respectively. The data are expressed as -fold increase over the basal level and are presented as the mean ± S.E. of three separate experiments. *, $p < 0.05$ versus cells transfected with control siRNA. H, effect of ARF1 siRNA on cAMP inhibition by α_{2B}-AR. HEK293 cells were transfected with α_{2B}-AR and control siRNA or ARF1 siRNA and stimulated with different concentrations of UK14,304 for 5 min as described in the legend for Fig. 4.

tively (Fig. 4E). In contrast, inhibition of forskolin-induced cAMP production in response to UK14,304 stimulation was very similar in cells expressing wild-type α_{2B}-AR and its diW motif mutant (Fig. 4H).

Effect of siRNA-mediated Knockdown of ARF1 on α_{2B}-AR-mediated ERK1/2 Activation—To further explore the role of ARF1 in α_{2B}-AR-mediated ERK1/2 activation, we determined the effect of siRNA-mediated depletion of endogenous ARF1 on the α_{2B}-AR-mediated ERK1/2 activation. Transient expression of ARF1 siRNA resulted in a marked reduction of endogenous ARF1 expression, but did not influence expression of the closely related small GTPase ARF3, demonstrating that ARF1 siRNA selectively knocks down ARF1 expression (Fig. 5, A and B). Transient expression of ARF1 siRNA did not significantly affect the cell surface and total expression of α_{2B}-AR (Fig. 5C).

Similar to the inhibitory effect of mutating the diW motif on α_{2B}-AR-mediated ERK1/2 activation, agonist dose- and time-dependent activation of ERK1/2 was consistently inhibited in cells expressing ARF1 siRNA (Fig. 5, D–G). The EC_{50} values were ∼0.016, 0.14, and 0.20 μM UK14,304 in cells transfected with control, ARF1 siRNA 1, and ARF1 siRNA 2, respectively (Fig. 5E). In contrast, siRNA-mediated knockdown of ARF1 did not clearly alter α_{2B}-AR-mediated inhibition of cAMP production induced by forskolin (Fig. 5H). These data demonstrate that ARF1 is required for maximal activation of ERK1/2, but not for inhibition of cAMP production, by α_{2B}-AR.

We then determined the effect of siRNA-mediated knockdown of ARF1 on the activation of ERK1/2 by endogenous α_{2B}-AR in MCF-7 cells. Expression of ARF1 siRNA did not influence the cell surface expression of endogenous α_{2B}-AR (Fig. 6A), but significantly reduced the activation of ERK1/2 in response to UK14,304 stimulation (Fig. 6, B and C) in MCF-7 cells. These data suggest that ARF1 participates in the modulation of ERK1/2 activation by endogenous α_{2B}-AR.

Activation of Raf1, MEK1, and ERK1/2 by the Activated Form of ARF1—We next asked whether or not enhancing ARF1 function could directly activate the Raf1-MEK1-ERK1/2 pathway. In the first series of experiments, we determined the effect of transient expression of ARF1 and its GTP-bound ARF1Q71L and GDP-bound ARF1T31N mutants on ERK1/2 activation. Expression of ARF1 moderately but significantly enhanced ERK1/2 activation, whereas ARF1Q71L markedly increased ERK1/2 activation (Fig. 7A).

ERK1/2 can be activated by a number of small GTPases, including Ras and ARF6 (39–42). In the second series of experiments, we compared the specificity and potency of these small GTPases in activating ERK1/2 in cells transfected with the same amount of plasmids. ERK1/2 activation was significantly elevated by the GTP-bound mutants of several small GTPases with the order Ras > ARF1 > ARF6 > ARF3 > ARF4. In contrast, transfection of the GTP-bound mutants of ARF5, Sar1, Rab1, Rab2, Rab4, Rab5, and Rab8 did not produce any clear effect on ERK1/2 activation (Fig. 7B). These data indicate that the active form of ARF1 is a potent activator of ERK1/2.

In the third series of experiments, we determined whether ARF1-mediated ERK1/2 activation could be modulated by transient expression of ARNO and ARFGAP1, which facilitate GDP-GTP exchange and GTP hydrolysis of ARF1, respectively
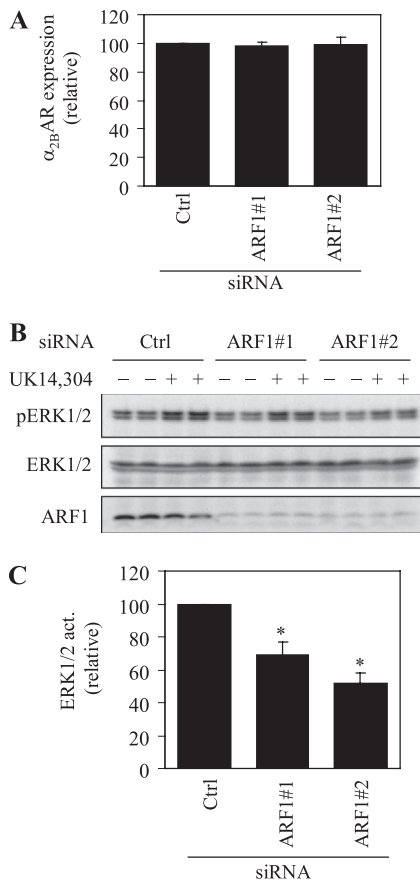
FIGURE 6. **Effect of siRNA-mediated ARF1 knockdown on ERK1/2 activation by endogenous α_2-AR in MCF-7 cells.** *A*, effect of ARF1 siRNA on the cell surface expression of α_2-AR. MCF-7 cells cultured on 6-well dishes were transiently transfected with control siRNA (*Ctrl*) or individual ARF1 siRNA, and the cell surface expression of α_2-AR was determined by intact cell ligand binding as described in the legend for Fig. 4. The data shown are percentages of the mean value obtained from cells transfected with control siRNA and are presented as the mean $\pm$ S.E. of three experiments. *B*, effect of ARF1 siRNA on ERK1/2 activation by endogenous α_2-AR. MCF-7 cells were transfected with control siRNA or individual ARF1 siRNAs (*ARF1#1* and *ARF1#2*) and stimulated with 0.1 μM UK14,304 for 5 min. *Upper panel*, a representative blot of ERK1/2 activation. *Middle panel*, total ERK1/2 expression. *Lower panel*, ARF1 expression. *C*, quantitation of data shown in *B*. The data shown are percentages of the mean value obtained from cells transfected with control siRNA and are presented as the mean $\pm$ S.E. of three different experiments. *, $p < 0.05$ *versus* cells transfected with control siRNA. *ERK1/2 act.*, ERK1/2 activation.

(43–45). Expression of ARNO further augmented ERK1/2 activation by ARF1 (Fig. 7C). The stimulatory effect of ARNO on ERK1/2 was partially inhibited by expression of ARFGAP1 (Fig. 7C).

In the fourth series of experiments, we defined whether the active form of ARF1 could activate the ERK1/2 upstream kinases MEK1 and Raf1. Expression of ARF1Q71L markedly activated both MEK1 (Fig. 8A) and Raf1 (Fig. 8B). Furthermore, ARF1Q71L-mediated ERK1/2 activation was dramatically inhibited by the dominant-negative Raf1 mutant K375M, but not the B-Raf1 mutant K482M (Fig. 8C). These data demonstrate that activation of ARF1 could activate the Raf1-MEK1-ERK1/2 pathway.

DISCUSSION

It has been well described that the functions of GPCRs are crucially regulated by their physical association with many reg-
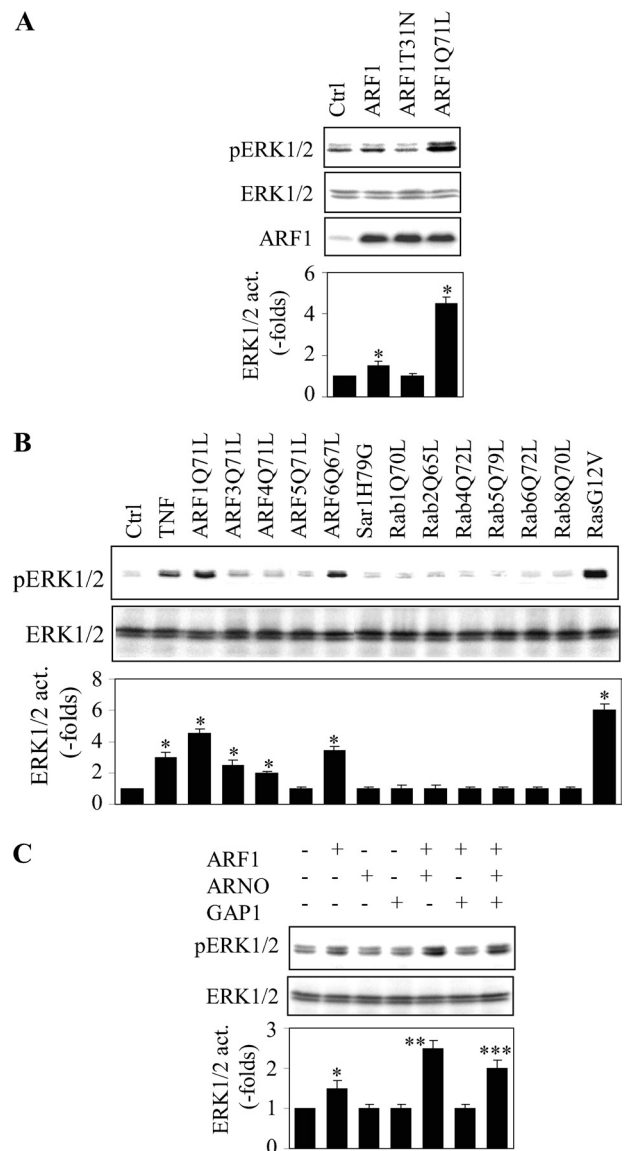

FIGURE 7. **Activation of ERK1/2 by the active form of ARF1.** *A*, ERK1/2 activation (*ERK1/2 act.*) by ARF1 and its GDP-bound ARF1T31N and GTP-bound ARF1Q71L mutants. HEK293 cells were transfected with the pcDNA3 vector, ARF1 or its mutants. ERK1/2 activation was measured by Western blotting measuring their phosphorylation using phospho-specific anti-ERK1/2 antibodies. *pERK1/2*, phosphorylated ERK1/2; *Ctrl*, control. *B*, comparison of ERK1/2 activation in HEK293 cells transfected with different GTP-bound small GTPase mutants. *C*, expression of ARNO augments ARF1-mediated ERK1/2 activation, and ARFGAP1 attenuates the ARNO effect on ERK1/2 activation. ARF1, ARNO, and ARFGAP1 were transiently expressed in HEK293 cells individually or in combination. ERK1/2 activation by tumor necrosis factor (TNF) is used as a control. In *A, B*, and *C*, quantitation of data shown in *bottom panels* is expressed as -fold increase over the basal level (control) and is presented as the mean $\pm$ S.E. of at least three separate experiments. *, $p < 0.05$ *versus* control. In *C*, ** and *** $p < 0.05$ *versus* ARF1 and ARF1 + ARNO, respectively.

ulatory proteins. In this study, we have first demonstrated that α_{2B}-AR and the small GTPase ARF1 can form a complex by co-immunoprecipitation and that the interaction between α_{2B}-AR and ARF1 was markedly potentiated by agonist stimulation. These data are consistent with other studies showing that GPCRs are able to associate with ARF GTPases (15, 35, 46, 47). Utilizing a GST fusion protein pulldown assay combined with progressive deletion and site-directed mutagenesis, we have further identified the diW motif in the membrane-proxi-
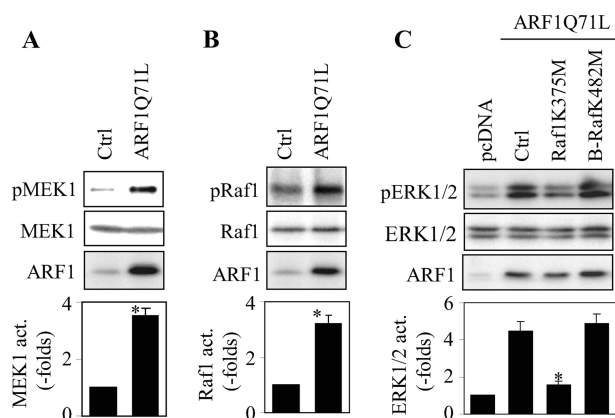
FIGURE 8. Activation of MEK1 and Raf1 by the active form of ARF1. *A*, activation of MEK1 by ARF1Q71L. *pMEK1*, phosphorylated MEK1; *Ctrl*, control. *B*, activation of Raf1 by ARF1Q71L. *pRaf1*, phosphorylated Raf1. *C*, expression of the dominant-negative mutant Raf1K375M, but not the B-RafK482M mutant, inhibits ERK1/2 activation by ARF1Q71L. HEK293 cells were transfected with ARF1Q71L alone or together with Raf1K375M or B-RafK482M. Activation of MEK1, Raf1, and ERK1/2 was measured by Western blotting measuring their phosphorylation using phospho-specific antibodies. *pERK1/2*, phosphorylated ERK1/2. Quantitation data shown in *bottom panels* are expressed as -fold increase over the basal level (control) and are presented as the mean ± S.E. of at least three individual experiments. In *A* and *B*, *, $p < 0.05$ *versus* control; in *C*, *, $p < 0.05$ *versus* pcDNA.

mal C-terminal region of the ICL3 as an ARF1-binding site, and mutation of the diW motif specifically and greatly attenuated agonist-promoted α_{2B}-AR interaction with ARF1. Analysis of the GPCR database reveals that the diW motif exists only in α_{2B}-AR. Therefore, the diW motif-mediated agonist-dependent α_{2B}-AR interaction with ARF1 is unique and very specific. Because other GPCRs have also been demonstrated to interact with ARF1 in response to agonist stimulation (46), it is possible that different GPCRs, when activated at the plasma membrane, may use distinct motifs to interact with ARF1. This agonist-dependent receptor-ARF1 interaction may be essential for the activation of a specific signal transduction pathway mediated by the receptor (*e.g.* ERK1/2 by α_{2B}-AR). In support of this possibility, the membrane-proximal C-terminal region of the ICL3 has been demonstrated to be responsible for the interaction of GPCRs with heterotrimeric G proteins and arrestins (30, 48, 49), which selectively associate with agonist-activated GPCRs.

However, mutation of the diW motif did not clearly influence α_{2B}-AR interaction with ARF1 in the absence of agonists. These data suggest that multiple ARF1-binding sites exist in α_{2B}-AR (36). Consistently, several GPCRs have been shown to use the ICL3 and/or the C termini to interact with ARF1 (35, 36, 50). It is possible that this agonist activation-independent ARF1-binding site is common to different GPCRs. As ARF1 has been well studied to function as an important transport regulator and to control the formation of COPI- and clathrin-coated vesicles that mediate cargo trafficking between multiple intracellular compartments, including the endoplasmic reticulum, the endoplasmic reticulum-Golgi intermediate compartment, the Golgi, the endosomes, and the plasma membrane (16–21), one possible function of the constitutive interaction between GPCRs and ARF1 is to modulate intracellular traffic of the receptors. Indeed, expression of dominant-negative mutants of ARF1 markedly inhibited the cell surface transport of all the GPCRs tested (36). Nevertheless, these studies strongly suggest

that the interaction between GPCRs and ARF1 may play multiple roles in the regulation of receptor biology.

The most important finding presented in this study is that the small GTPase ARF1 is involved in the regulation of the MAPK signaling pathway, specifically the activation of ERK1/2 by α_{2B}-AR. We have demonstrated that mutation of the diW motif to disrupt α_{2B}-AR interaction with ARF1 clearly attenuated the ability of the receptor to activate ERK1/2, but not to inhibit cAMP production, suggesting that the diW motif-mediated α_{2B}-AR-ARF1 interaction is specifically required for the maximal activation of ERK1/2 by the receptor. The fact that the mutation of the diW motif did not significantly alter α_{2B}-AR cell surface transport and endocytosis in response to agonist stimulation implies that the diW motif-mediated α_{2B}-AR interaction with ARF1 is unlikely to be involved in the regulation of intracellular trafficking of α_{2B}-AR. Indeed, ARF6, but not ARF1, has been demonstrated to be involved in regulation of GPCR internalization (51, 52). Therefore, the signaling defect in activating MAPK observed in the diW mutant is not due to altered receptor expression at the cell surface *per se*.

Consistent with the role of ARF1 in α_{2B}-AR-mediated activation of ERK1/2, siRNA-mediated depletion of ARF1 attenuated partially but significantly time- and agonist dose-dependent activation of ERK1/2. siRNA-mediated knockdown of ARF1 also reduced the activation of ERK1/2 by endogenous α_{2B}-AR in MCF-7 cells. The partial inhibition of α_{2B}-AR-mediated activation of ERK1/2 induced by mutating the ARF1-binding diW motif and ARF1 siRNA is in agreement with previous studies demonstrating that multiple players such as heterotrimeric G proteins and Ras are involved in α_{2B}-AR-mediated ERK1/2 activation (9, 10). It is interesting to note that siRNA-mediated knockdown of ARF1 did not influence the cell surface expression of exogenously expressed α_{2B}-AR in HEK293 cells and endogenous α_{2B}-AR in MCF-7 cells. Our previous studies have demonstrated that inhibition of ARF1 functions via expression of the dominant-negative, GDP-bound mutant ARF1T31N, which markedly inhibited both α_{2B}-AR transport to the cell surface and α_{2B}-AR-mediated ERK1/2 activation (36). These data suggest that ARF1 and other ARF GTPases, particularly ARF3, which is in the same class may have overlapping and redundant functions in the cell surface export of α_{2B}-AR. Consistent with this possibility, siRNA-mediated knockdown of any individual ARF GTPase did not produce significant influence on membrane traffic (38).

The data presented here suggest a novel function for ARF1 in regulating the activation of the MAPK signaling pathway. It has been well characterized that the small GTPase Ras is a very strong activator for the Raf1-MEK1-ERK1/2 pathway. It has also been shown that ARF6 can activate ERK1/2, which plays a vital role in tumor cell invasion (40). We have demonstrated here that expression of constitutively active, GTP-bound ARF1Q71L mutant markedly activated Raf1, MEK1, and ERK1/2. Among the five ARFs, ARF1 is the strongest activator of ERK1/2. Expression of GTP-bound mutants of ARF3 and ARF4 also activated ERK1/2, but at much lower magnitudes. Furthermore, facilitation of GDP exchange for GTP through ARNO expression enhanced ERK1/2 activa-

tion, which can be reversed by promoting GTP hydrolysis of ARF1 via expressing ARFGAP1. These data indicate that the active from of ARF1 is a potent activator of the Raf1-MEK1-ERK1/2 pathway. It is interesting to note that ARNO is required for the sustained activation of ERK1/2 by the A2A adenosine receptor (43). Whether or not ARNO is also involved in the regulation of α_{2B}-AR/ARF1-mediated ERK1/2 activation is under investigation. Nevertheless, the data presented in this study, together with other studies demonstrating that ARF1 directly activates signaling molecules such as phospholipase D (22, 23), strongly indicate that, in addition to its well established function as a traffic coordinator, ARF1 GTPase also functions as a signal transducer regulating the MAPK signaling pathway.

In the conventional GPCR signaling pathways, GPCRs directly relay the signals by activating α and $\beta\gamma$ subunits of heterotrimeric G proteins. It is now well known that GPCRs can also activate small GTPases, such as Ras, to regulate the MAPK signaling pathway. Here we demonstrate that α_{2B}-AR-mediated ERK1/2 activation depends at least partially on the small GTPase ARF1. These data also suggest a novel MAPK activation pathway involving ARF1 in which α_{2B}-AR activates ERK1/2. The function of ARF1 in regulating α_{2B}-AR-mediated ERK1/2 activation is likely dictated by its unique interaction with the receptor. Because the activation of the MAPK pathway regulates a number of cellular functions under physiological and pathological conditions, the molecular mechanism underlying ERK1/2 activation by α_{2B}-AR and ARF1 merits further investigation.

REFERENCES

1. Pierce, K. L., Premont, R. T., and Lefkowitz, R. J. (2002) *Nat. Rev. Mol. Cell Biol.* **3,** 639–650
2. Wess, J. (1998) *Pharmacol. Ther.* **80,** 231–264
3. Schmitt, J. M., and Stork, P. J. (2000) *J. Biol. Chem.* **275,** 25342–25350
4. Goldsmith, Z. G., and Dhanasekaran, D. N. (2007) *Oncogene* **26,** 3122–3142
5. Lee, M. H., El-Shewy, H. M., Luttrell, D. K., and Luttrell, L. M. (2008) *J. Biol. Chem.* **283,** 2088–2097
6. Lefkowitz, R. J., Rajagopal, K., and Whalen, E. J. (2006) *Mol. Cell* **24,** 643–652
7. Luo, J., Busillo, J. M., and Benovic, J. L. (2008) *Mol. Pharmacol.* **74,** 338–347
8. Williams, N. G., Zhong, H., and Minneman, K. P. (1998) *J. Biol. Chem.* **273,** 24624–24632
9. DeGraff, J. L., Gagnon, A. W., Benovic, J. L., and Orsini, M. J. (1999) *J. Biol. Chem.* **274,** 11253–11259
10. Cussac, D., Schaak, S., Denis, C., and Paris, H. (2002) *J. Biol. Chem.* **277,** 19982–19988
11. D'Souza-Schorey, C., and Chavrier, P. (2006) *Nat. Rev. Mol. Cell Biol.* **7,** 347–358
12. Roth, M. G. (1999) *Cell* **97,** 149–152
13. Hiroi, T., Someya, A., Thompson, W., Moss, J., and Vaughan, M. (2006) *Proc. Natl. Acad. Sci. U.S.A.* **103,** 10672–10677
14. Palacios, F., Price, L., Schweitzer, J., Collard, J. G., and D'Souza-Schorey, C. (2001) *EMBO J.* **20,** 4973–4986
15. Madziva, M. T., and Birnbaumer, M. (2006) *J. Biol. Chem.* **281,** 12178–12186
16. Spang, A. (2002) *Curr. Opin. Cell Biol.* **14,** 423–427
17. Stearns, T., Willingham, M. C., Botstein, D., and Kahn, R. A. (1990) *Proc. Natl. Acad. Sci. U.S.A.* **87,** 1238–1242
18. Balch, W. E., Kahn, R. A., and Schwaninger, R. (1992) *J. Biol. Chem.* **267,** 13053–13061
19. Misra, S., Puertollano, R., Kato, Y., Bonifacino, J. S., and Hurley, J. H. (2002) *Nature* **415,** 933–937
20. Puertollano, R., Randazzo, P. A., Presley, J. F., Hartnell, L. M., and Bonifacino, J. S. (2001) *Cell* **105,** 93–102
21. Bonifacino, J. S. (2004) *Nat. Rev. Mol. Cell Biol.* **5,** 23–32
22. Cockcroft, S., Thomas, G. M., Fensome, A., Geny, B., Cunningham, E., Gout, I., Hiles, I., Totty, N. F., Truong, O., and Hsuan, J. J. (1994) *Science* **263,** 523–526
23. Brown, H. A., Gutowski, S., Moomaw, C. R., Slaughter, C., and Sternweis, P. C. (1993) *Cell* **75,** 1137–1144
24. Roth, M. G. (2008) *Traffic* **9,** 1233–1239
25. Massenburg, D., Han, J. S., Liyanage, M., Patton, W. A., Rhee, S. G., Moss, J., and Vaughan, M. (1994) *Proc. Natl. Acad. Sci. U.S.A.* **91,** 11718–11722
26. Zhang, G. F., Patton, W. A., Lee, F. J., Liyanage, M., Han, J. S., Rhee, S. G., Moss, J., and Vaughan, M. (1995) *J. Biol. Chem.* **270,** 21–24
27. Wu, G., Zhao, G., and He, Y. (2003) *J. Biol. Chem.* **278,** 47062–47069
28. Dong, C., and Wu, G. (2006) *J. Biol. Chem.* **281,** 38543–38554
29. Duvernay, M. T., Wang, H., Dong, C., Guidry, J. J., Sackett, D. L., and Wu, G. (2011) *J. Biol. Chem.* **286,** 14080–14089
30. Wu, G., Krupnick, J. G., Benovic, J. L., and Lanier, S. M. (1997) *J. Biol. Chem.* **272,** 17836–17842
31. Wu, G., Benovic, J. L., Hildebrandt, J. D., and Lanier, S. M. (1998) *J. Biol. Chem.* **273,** 7197–7200
32. Dong, C., Yang, L., Zhang, X., Gu, H., Lam, M. L., Claycomb, W. C., Xia, H., and Wu, G. (2010) *J. Biol. Chem.* **285,** 20369–20380
33. Filipeanu, C. M., Zhou, F., Claycomb, W. C., and Wu, G. (2004) *J. Biol. Chem.* **279,** 41077–41084
34. Dong, C., and Wu, G. (2007) *Cell. Signal.* **19,** 2388–2399
35. Mitchell, R., Robertson, D. N., Holland, P. J., Collins, D., Lutz, E. M., and Johnson, M. S. (2003) *J. Biol. Chem.* **278,** 33818–33830
36. Dong, C., Zhang, X., Zhou, F., Dou, H., Duvernay, M. T., Zhang, P., and Wu, G. (2010) *J. Pharmacol. Exp. Ther.* **333,** 174–183
37. Kumari, S., and Mayor, S. (2008) *Nat. Cell Biol.* **10,** 30–41
38. Volpicelli-Daley, L. A., Li, Y., Zhang, C. J., and Kahn, R. A. (2005) *Mol. Biol. Cell* **16,** 4495–4508
39. Chiu, V. K., Bivona, T., Hach, A., Sajous, J. B., Silletti, J., Wiener, H., Johnson, R. L., 2nd, Cox, A. D., and Philips, M. R. (2002) *Nat. Cell Biol.* **4,** 343–350
40. Tague, S. E., Muralidharan, V., and D'Souza-Schorey, C. (2004) *Proc. Natl. Acad. Sci. U.S.A.* **101,** 9671–9676
41. Tushir, J. S., and D'Souza-Schorey, C. (2007) *EMBO J.* **26,** 1806–1819
42. Vojtek, A. B., Hollenberg, S. M., and Cooper, J. A. (1993) *Cell* **74,** 205–214
43. Gsandtner, I., Charalambous, C., Stefan, E., Ogris, E., Freissmuth, M., and Zezula, J. (2005) *J. Biol. Chem.* **280,** 31898–31905
44. Yang, J. S., Lee, S. Y., Gao, M., Bourgoin, S., Randazzo, P. A., Premont, R. T., and Hsu, V. W. (2002) *J. Cell Biol.* **159,** 69–78
45. Cukierman, E., Huber, I., Rotman, M., and Cassel, D. (1995) *Science* **270,** 1999–2002
46. Mitchell, R., McCulloch, D., Lutz, E., Johnson, M., MacKenzie, C., Fennell, M., Fink, G., Zhou, W., and Sealfon, S. C. (1998) *Nature* **392,** 411–414
47. Deretic, D., Williams, A. H., Ransom, N., Morel, V., Hargrave, P. A., and Arendt, A. (2005) *Proc. Natl. Acad. Sci. U.S.A.* **102,** 3301–3306
48. Wade, S. M., Scribner, M. K., Dalman, H. M., Taylor, J. M., and Neubig, R. R. (1996) *Mol. Pharmacol.* **50,** 351–358
49. DeGraff, J. L., Gurevich, V. V., and Benovic, J. L. (2002) *J. Biol. Chem.* **277,** 43247–43252
50. Robertson, D. N., Johnson, M. S., Moggach, L. O., Holland, P. J., Lutz, E. M., and Mitchell, R. (2003) *Mol. Pharmacol.* **64,** 1239–1250
51. Claing, A., Chen, W., Miller, W. E., Vitale, N., Moss, J., Premont, R. T., and Lefkowitz, R. J. (2001) *J. Biol. Chem.* **276,** 42509–42513
52. Houndolo, T., Boulay, P. L., and Claing, A. (2005) *J. Biol. Chem.* **280,** 5598–5604